

ORDEM 4.0: NASA'S ORBITAL DEBRIS ENGINEERING MODEL — A STATUS

Mark Matney⁽¹⁾, Andrew Vavrin⁽²⁾, Michael Poehlmann⁽³⁾, Austen King⁽⁴⁾, John H. Seago⁽⁵⁾,
Phillip Anz-Meador⁽⁴⁾, Jer-Chyi Liou⁽¹⁾, Corbin Cruz⁽⁴⁾, Alyssa Manis⁽¹⁾

⁽¹⁾ NASA Orbital Debris Program Office, NASA Johnson Space Center, Mail Code XI5-9E,
2101 NASA Parkway, Houston, TX 77058, USA

⁽²⁾ GeoControl Systems, Amentum JETS II Contract, NASA Johnson Space Center, Mail Code JS24,
Houston, TX 77058, USA

⁽³⁾ Intuitive Machines, Amentum JETS II Contract, NASA Johnson Space Center, Mail Code JS24,
Houston, TX 77058, USA

⁽⁴⁾ Amentum Services, Inc., NASA Johnson Space Center, Mail Code JS24, Houston, TX 77058, USA

⁽⁵⁾ Astrion, Amentum JETS II Contract, NASA Johnson Space Center, Mail Code JS24,
Houston, TX 77058, USA

ABSTRACT

For over three decades, the NASA Orbital Debris Program Office (ODPO) has been developing the Orbital Debris Engineering Model (ORDEM) to provide satellite users and designers the resources necessary to compute collision risks from orbital debris. Iterations of this model compute information on the debris flux rates, direction, speed, size, and material densities based on the spacecraft asset's orbit and predict the flux up to several decades in the future to encompass the time these spacecraft plan to operate. Engineering models need to be updated periodically as the environment and launch traffic changes (often in unpredictable ways). In addition, measurements, analysis techniques, and knowledge of the nature of orbital debris are constantly being improved, allowing the development of new capabilities.

The ORDEM 3 series are the most recent releases of the ORDEM model. They describe the debris flux in terms of material density of the debris in five categories: low-density (*e.g.*, plastic), medium-density (*e.g.*, aluminum), high-density (*e.g.*, steel), intact objects, and the sodium-potassium (NaK) population. The material density is a significant parameter in determining which size debris will cause a given level of damage. Additionally, the outputs include an estimate of the uncertainties in the debris populations. The current version, ORDEM 3.2, was updated in 2022 to include the large debris cloud from the deliberate breakup of the Cosmos 1408 satellite on 15 November 2021.

This paper will describe the development and status of the newest ORDEM model, ORDEM 4.0. As with other ORDEM models, ORDEM 4.0 will include populations based on the most recent data from ground-based telescopes and radars as well as *in situ* measurements. The most important update, however,

will be the inclusion of debris shapes, as this is another crucial parameter in determining how debris impacts damage surfaces. Extensive study of the recovered debris shapes from the DebrisSat and prior experiments has allowed the ODPO to develop a simple model to parameterize the shapes as right circular cylinders. While this abstraction does not fully encompass all possible debris shape effects, these simplified shapes represent a major improvement in how damage is tested and computed. Further, a number of improved techniques have been introduced to model the debris populations; therefore, we will present the updated populations included in ORDEM 4.0 and how they compare to previous versions of ORDEM.

1 INTRODUCTION

The NASA Orbital Debris Program Office (ODPO) began development of the Orbital Debris Engineering Model (ORDEM) in the mid-1980s in support of the Space Station Program Office. The ORDEM software currently serves as the primary tool to provide a timely, validated model of the human-made orbital debris environment. It facilitates modeling assessments by spacecraft owners/operators, as well as ground-based observation planning. Early versions of the model were based on analytical formulae representing the debris environment [1]. The first computer-based version of ORDEM was released in 1996 as ORDEM96 and pioneered the use of debris population ensembles characterized by altitude, eccentricity, inclination, and size [2]. ORDEM2000 replaced the curve-fitting approach with a finite element representation of the debris environment [3]. ORDEM 3.0 represented a significant upgrade in terms of model features and capabilities [4]. It extended the model to the geosynchronous orbit (GEO) region (up to 40,000 km), which enabled

analysis of more varied orbits – such as geosynchronous transfer orbits (GTO) and other highly elliptical spacecraft orbits – and sensor orientations. Additional upgrades included expansion of observation program datasets in underrepresented regions and the addition of uncertainties on the reported orbital debris flux. Most significantly, ORDEM 3.0 included a distribution in material density of orbital debris fluxes [5].

The orbital debris environment is dynamic; therefore, the models need to be periodically updated. As newer datasets become available, they provide more information on the evolution of the orbital debris environment. In addition, newly developed data analysis techniques can be applied to both new and legacy data to improve the assessment of orbital debris populations. ORDEM 3.1 was created to include the same capabilities as ORDEM 3.0 and to incorporate updated datasets available to NASA for both constructing and validating the modeled orbital debris populations [6]. New approaches to analyzing the available data were also implemented for the large breakup clouds (*Fengyun-1C* [FY-1C], Iridium 33, and Cosmos 2251), *in situ* impact data, and the GEO population.

On 15 November 2021, the Russian Federation tested a direct-ascent anti-satellite weapon on their Cosmos 1408 spacecraft [7]. The resulting large cloud of debris was of sufficient size and concern that the ODPO created an update of the ORDEM model (ORDEM 3.2) to include the effects of this new cloud. This update was released in early 2022 [8].

For the next generation of ORDEM models – ORDEM 4.0 – several changes have been implemented. The most important change is the inclusion of debris shape. Other updates include expanded density families, a new approach to binning debris populations (both spatially and by size), and as with previous versions, more recent datasets for building and validating model populations.

2 DEBRIS SHAPE

Multiple NASA reviews of the ORDEM model through the years indicated a major limitation was the over-simplification of the shape model – all objects were assumed to be spheres, as was assumed in all ORDEM models.

The most important change for ORDEM 4.0 will be a debris shape model. This effort has been aided by the unprecedented level of detail in the analysis of the DebrisSat debris fragments, including shape information [9, 10]. A difficult problem in attempting to parameterize shape is the complexity of ensuring consistency of shape, dimensions, volume, mass, and mass density or “effective” density.

One possible debris shape with axial symmetry is a prolate or oblate spheroid. This has the benefit of being a variation on a sphere; however, the manufacture of these shapes for hypervelocity impact tests has proven difficult, especially for small impactors [11]. Instead, for ORDEM 4.0 the shape with axial symmetry chosen is a right circular cylinder (RCC), defined by its length-to-diameter ratio (L:D). A cylinder with $L:D > 1$ is a rod shape, and one with $L:D < 1$ is more disk-like. This shape is relatively easy to manufacture by cutting cylindrical rods or wires of material. The actual “shoehorning” of various debris shapes into these categories is a complex subject [9], but it allows debris shapes to be parameterized and stored in a computer model in a tractable fashion.

L:D ratios for the DebrisSat fragments span a continuum of values, from long rods, to nugget-like squat cylinders, to plate-like debris. To simplify the model storage of shape information, the model takes advantage of the fact that the debris falls into broad groupings of L:D ratios with distributions that are generally log-normal in nature (Fig. 1). In the model, these L:D ratios are grouped by a single, size-independent median value and associated standard deviation of L:D to define an entire shape sub-family.

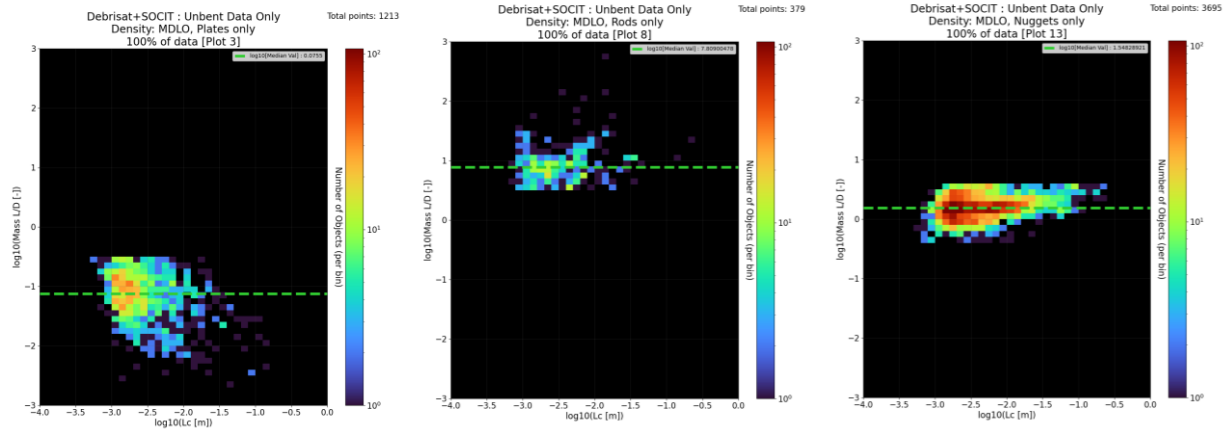


Figure 1. Example L:D distributions of the Medium-Low density composite population (MDLO – corresponding mostly to aluminum particles) for three size groupings based on SOCIT and Debrisat data. As can be seen, the distributions in logarithmic shape parameters are mostly independent of size, and can be estimated as log-normal in L:D ratio, with a median defined by the green dotted lines.

While these assumptions may seem to oversimplify a complex shape distribution, it is useful to keep in mind that there is currently no engineering model for orbital debris that explicitly includes shape. Parameterizing shape represents a significant achievement in capability and accuracy. Therefore, these RCCs mark a major improvement in the ability to compute probabilistic debris risk.

One challenge with testing non-spherical shapes in a hypervelocity impact test facility is that in practice it is impossible to control the flight angle of non-spherical shapes as they hit the target. However, instead of trying to control the orientation of the projectile, cameras can be used to measure the randomized orientation as the impactor hits. Using several tests with various measured random orientations allows the analyst to calibrate the damage hydrocodes and determine a damage equation for an expanded set of orientations of the RCC [11]. These damage equations are then referenced to those determined by impacts with spherical debris (analogous to L:D ~1) to come up with a comprehensive shape-dependent function. There are limitations, however, as very long rods and very thin disks are difficult to test in the lab and compute using hydrocodes. Nevertheless, with only a modicum of new tests with RCCs, new, improved damage equations can be formulated that leverage work already done with spherical debris.

3 MODEL CHANGES

3.1 Density Families

One of the findings in analyzing the U.S. Space Transportation System (STS), the Space Shuttle, data for the ORDEM models was the presence of titanium debris in the Shuttle returned surfaces, assessed as metal rather than paint pigment. Titanium has a density of 4.5 g/cm^3 , which places it midway between the previous categories of Medium Density (aluminum, 2.8 g/cm^3 , being representative) and High Density (stainless steel, 7.9 g/cm^3 , being representative). In recognition of this non-trivial component of the environment, Medium Density is now divided into two density classes Medium-Low Density ($2\text{-}4 \text{ g/cm}^3$) and Medium-High Density ($4\text{-}6 \text{ g/cm}^3$).

Another new class of material density has been introduced by the analysis of the Debrisat data [10]. The target, a high fidelity mock satellite, was deliberately created to be representative of more modern spacecraft in low Earth orbit (LEO), so it included large amounts of carbon fiber-reinforced plastic (CFRP), with density 1.46 g/cm^3 . As this debris population has a singular density within the Low Density category ($0\text{-}2 \text{ g/cm}^3$), plus exhibiting unique shape characteristics, it is now incorporated as its own density class for ORDEM 4.0.

3.2 Size Binning

One of the features of the ORDEM 3 family of models is that the size distributions were divided into half-decade bins for storage and computation purposes. Careful analysis showed that doubling the

number of size bins to four per decade in size, from 10- μm to 1 m, provides a better model for the inflection points in the size distributions of the various populations contributing to the total flux at all sizes.

A careful study was done with ORDEM 4.0 to determine if size (Characteristic Length [12]) was still a useful model parameter, or if it would be more appropriate to switch to another parameter, such as mass. After much discussion, the ODPO determined there was no major technical benefit to using one parameter over another. Therefore, the decision was made to stay with a size parameterization for consistency with past and current models, guidelines, and requirements.

3.3 Igloo Binning

One inefficiency with previous ORDEM models is the binning of the IGLOO file – the breakdown of the debris flux in terms of a two-dimensional direction and relative velocity in the spacecraft frame. Previously, binning in equal displacements in azimuth and elevation was used, but this meant that the model was computationally expensive and used excessive storage allocation computing fluxes near the poles (typically the nadir and zenith directions), while most of the debris flux occurs (at least for circular orbits) in the local horizontal plane (the “equator” of the IGLOO). After examining several options, a formulation of the IGLOO that preserves solid angle was adopted using the method of Arvo [13]. The Arvo method maps squares on a cube onto a unit sphere in such a way that each of the elements has the same solid angle and area on the unit sphere (Fig. 2). This method is much more

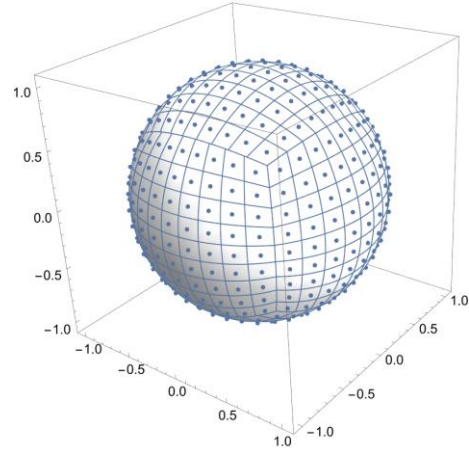


Figure 2. The final Arvo map is composed of mapping all six sides of the cube. Each of the elements subtend the same solid angle.

versatile in that it can handle any flux direction pattern, while saving in computation time and storage.

4 ORDEM 4.0 MODEL POPULATIONS

The core feature of the ORDEM series of orbital debris environment models is their reliance on empirical data, and reliable data are required to build a realistic and valid model. Tab. 1 summarizes the ground-based and *in situ* datasets used for building and validating the ORDEM 4.0 model, including their respective calendar year (CY) range of measurements. To place these measurements in context with regard to ORDEM 3.1/3.2, Tab. 2 contrasts population build sets used for ORDEM 3.1 [6] and ORDEM 4.0.

Table 1. Datasets used for building and validating the ORDEM 4.0 model populations.

Data Source	Year(s) of Coverage – Build	Year(s) of Coverage – Validation
SSN Catalog	1957–2022	2023 and after
HUSIR (Haystack Ultrawideband Satellite Imaging Radar)	2016–2022	2023 and after
HAX (Haystack Auxiliary Radar)	2018–2020	N/A (no data available after 2020)
Goldstone Orbital Debris Radar	N/A	2016–2017
STS windows and radiators	1995–2011	N/A
HST WFPC2 (Wide Field and Planetary Camera 2)	N/A	1993–2009
ES-MCAT (Eugene Stansbery – Meter Class Autonomous Telescope)	N/A	2023
MODEST (Michigan Orbital DEbris Survey Telescope)	2004–2006, 2007–2009, 2013–2014	N/A
HST MLI (Hubble Space Telescope Multi-Layer Insulation)	N/A	1990–2009
PMA-2 cover (Pressurized Mating Adapter 2)	N/A	2013–2015

Table 2. Datasets contrasted: the annual coverage of ground-based and in situ data used to build the ORDEM 3.1 and 4.0 models, including relevant size limits.

Data Source		Size Limit(s)	Years covered ORDEM 3.1	Years covered ORDEM 4.0
In situ	STS radiators and windows	10 μ m – 1 mm	1995–2011	1995–2011
Radar	Goldstone	3 – 8 mm	N/A	2016–2022
	HUSIR 75E	>5.5 mm	2013–2015	2016–2022
	HUSIR 20S	>5.5 mm	2015	2016–2022
	HAX 75E	>3 cm	N/A	2018–2020
	SSN Catalog	>10 cm (LEO)	1957–2014 (LEO)	1957–2022
		>1 m (GEO)	1957–2015 (GEO)	
Optical	MODEST	30 cm – 1 m	2004–2006, 2007–2009	2004–2006, 2007–2009, 2013–2014
	ES-MCAT	30 cm – 1 m	N/A	N/A

The fundamental dataset for ODPO modeling efforts is the ODPO-maintained space traffic database, which characterizes satellites launched – including known and/or estimated orbital elements and physical characteristics – as well as details of known historical breakups and maneuvers. The space traffic database is largely predicated upon the U.S. Space Surveillance Network (SSN) catalog, which is considered nearly complete for objects larger than approximately 10 cm in LEO and 1 m in geosynchronous orbit (GEO). The yearly space traffic is propagated forward in time using the NASA low Earth orbit (LEO)-to-GEO Environment Debris (LEGEND) model [14]. The LEGEND model provides the baseline for most sub-populations in ORDEM. The historical population (*i.e.*, initial reference population) for ORDEM 4.0 covers launches from 1957 to 2022 inclusive.

Fragments from confirmed historical fragmentation events down to 1 mm in size were created using a

special in-house version of the NASA SSBM incorporating preliminary debris shape data based on laboratory impact tests, including fragment characteristics, material density, and shape. For future projection, objects were added to the population assuming a repeat of the previous 8-year launch traffic cycle and a post-mission disposal success rate of 90% for rocket bodies and spacecraft. Future collisions and explosions were modeled statistically. Objects greater than 10 cm were allowed to collide according to the “cube” collision assessment algorithm in LEGEND [15]. Probabilities of explosion for intact objects were assessed using an empirical time-dependent explosion rate model. To build a statistically complete representation of debris populations, the initial reference population was adjusted based on data from instruments optimized to observe debris with sizes smaller than the SSN cataloging threshold, including ground-based and *in situ* sensors.

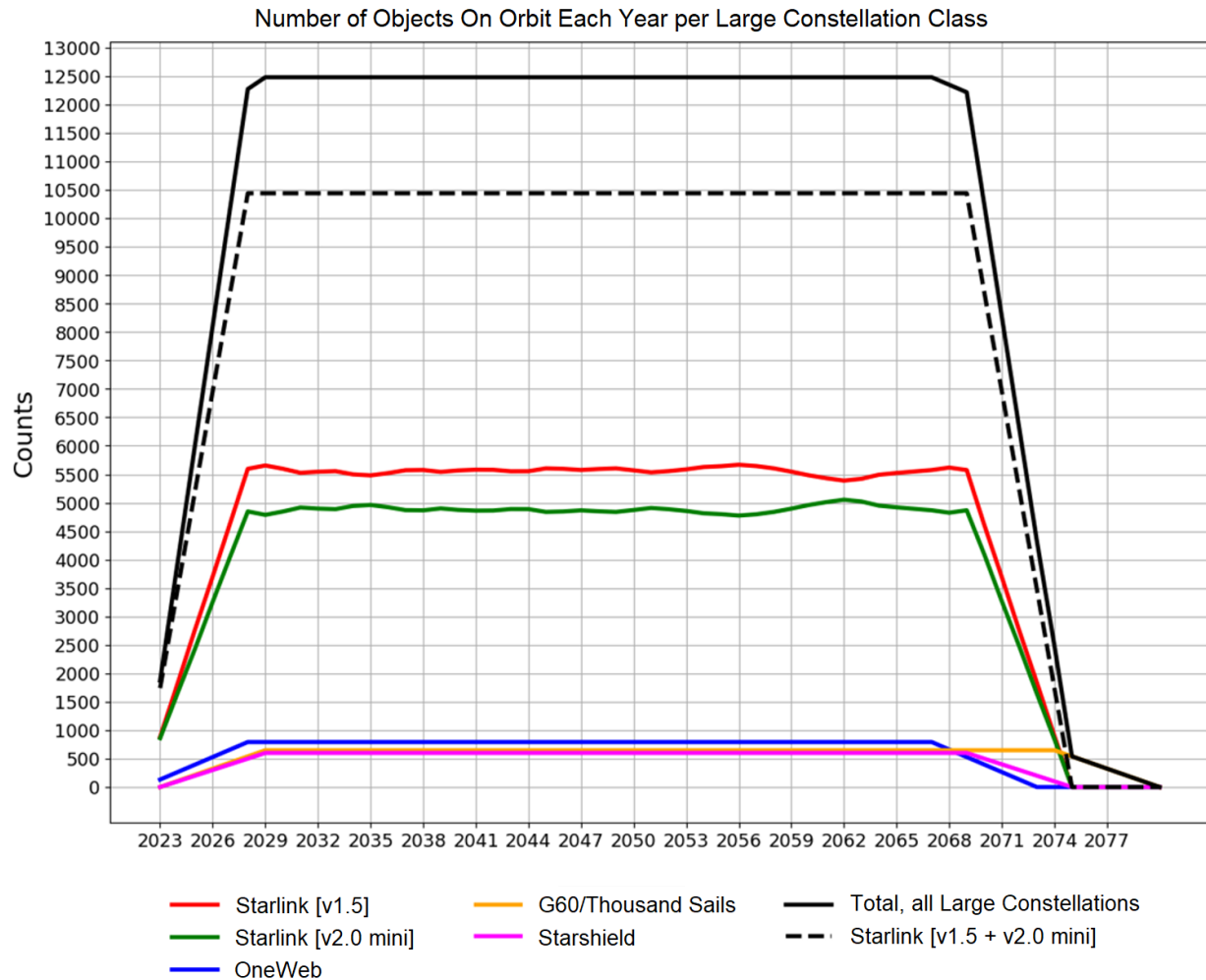


Figure 3. This chart shows the large satellite constellations simulated for ORDEM 4.0, with build-up times and (assumed) disposal after 50 years of service per constellation. The Starlink satellites are divided into two bus variants, as well as the Starshield variant. The G60/Thousand Sails refers to the Chinese constellation. The dashed line is the sum of the red and green Starlink bus variant lines.

An important addition to ORDEM 4.0 is the incorporation of large constellations and their subsequent influence upon the environment. This is a subject of dynamic change as new constellations are proposed and deployed. This dynamism created challenges to predicting and modeling these constellations for the future. For ORDEM, the constellations were modeled to do collision avoidance during their operational lifetimes and have a 99% chance of performing successful PMD at the end of life. In addition, the constellations were assumed to have a zero rate of explosions.

The constellations would thus contribute to the debris population in two ways. The first is future collisions where one of the objects is an inert constellation member that failed PMD. The second is the production

of small debris (see Section 4.2). Because of the large, combined areas of these complexes of satellites, the small debris production is not trivial. A total of 5 constellations were included in the model, as seen in Fig. 3.

While the launch rates, lifetimes, orbits, physical areas, and projected total numbers of these constellations are sometimes poorly known, we believe this model captures a reasonable estimate of expected future behaviors over the next few decades based on our current level of knowledge. The constellation model will be revised and updated on a regular basis.

4.1 Radar-based Populations

The Haystack Ultrawideband Satellite Imaging Radar (HUSIR) and Goldstone Orbital Debris Radar are the primary sources of radar data utilized by the ODPO [16]. HUSIR (previously Haystack) is a 37 m dish, monostatic X-band radar operated by the Massachusetts Institute of Technology Lincoln Laboratory, which provides data for LEO debris larger than approximately 5.5 mm. Goldstone, a bistatic

X-band radar, is operated by NASA's Jet Propulsion Laboratory (JPL). It uses a 70 m- and 34 m-diameter dish for the transmit and receive antennas, respectively, and extends LEO coverage of debris down to approximately 2-3 mm. Both HUSIR and Goldstone operate in a staring mode for debris observations, pointed at a fixed point in space with respect to the local topocentric coordinate system while objects pass through the radar beam.

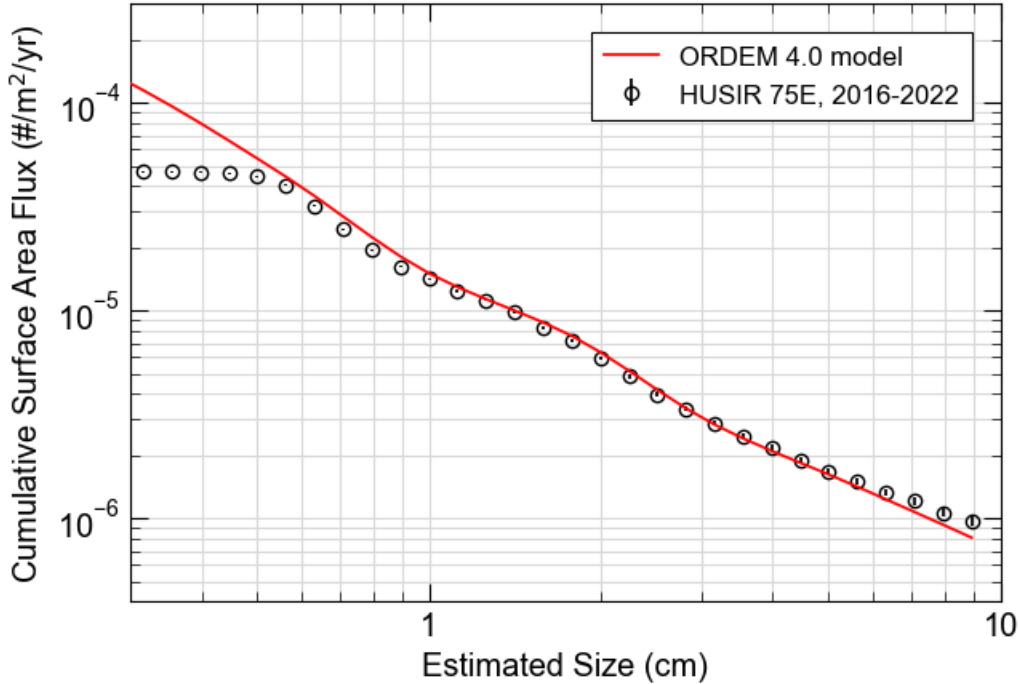


Figure 4. ORDEM 4.0 fits obtained by scaling the model populations to predict the detection rate of HUSIR data over a 7-year time span (in this case, LEO HUSIR data). Overall, the fitting accurately reflects the complex radar data at different sizes, inclinations, and altitudes.

Composite data from HUSIR over CY2016–2022 were used to scale the initial LEO populations modeled by LEGEND (Fig. 4). This is accomplished by using a detection space of binned values of radar cross section, range, and Doppler range-rate. The LEGEND population is then “flown” through a modeled HUSIR beam to compute the detection rate in each of these detection bins. The LEGEND populations are then adjusted in number at each size to better match the actual HUSIR detections using a maximum likelihood estimation. In principle, such a fitting should be straightforward, but because the population is a complex multidimensional distribution, parameterization of the populations must be carefully constructed to give reasonable results.

Because the Goldstone radar does not correct for the path through the beam using monopulse as does HUSIR, the Goldstone data proved much more difficult to use in the automated fitting procedure. In addition, new pointing modes for Goldstone have created new challenges to interpreting the data [17]. New techniques to analyze Goldstone data are being developed and used for validation of the populations, especially below the HUSIR lower size limit of approximately 5 mm.

4.2 In Situ-based Populations

Data for building the ORDEM 4.0 debris population in the sub-millimeter size range in LEO are provided by the database of impacts to the STS orbiter vehicle (Shuttle), as archived by NASA's Hypervelocity Impact Technology group. The database contains information

on impacts to the Shuttle, categorized by mission and surface. Data on impacts to the Shuttle windows (excluding the cargo bay windows) and radiators from STS missions 71 through 133 (1995-2011) were again used for building the ORDEM 4.0 small particle population [18]. The STS window and radiator data approximately cover size ranges of 10 μm – 300 μm and 300 μm – 1 mm, respectively. In many cases, electron microscope analysis of residue in the damage features enabled the identification of the type of impactor (*e.g.*, meteoroid, steel, aluminum, etc.). Unfortunately, no analogous high-quality, large area sensors have provided *in situ* data since the cessation of the Shuttle program in 2011, so this data is still an important contributor to ORDEM 4.0, despite its vintage.

Since the time this data was used to fit the ORDEM 3.1 model [19, 20], several important changes have occurred in modeling of these populations. First, new mathematical techniques have been developed that enhance the ability to fit the data. With the addition of the new density classes and shape modeling, the manner in which the data is parsed and the damage equations applied needed to be updated.

As in ORDEM 3.1, the small particle population less than approximately 3 mm was modeled separately from the radar-based population using a special small-particle degradation model [21] that creates small particles assuming a production rate proportional to the surface area of a source body. The average production rate was calculated using an arbitrary initial production rate based on particle size, time interval, and the surface area of the source object. The initial size distribution was sampled randomly from a uniform distribution (in Log_{10} space) between 10 μm and 3 mm.

In ORDEM 3.1, the model was agnostic with respect to the production mechanism for these small particles,

and it was assumed they were created with zero relative velocity to the parent body, with production rate proportional to the area of the parent. Over time the ODPO has concluded that these small particles are produced by ejecta from hypervelocity impacts and space weathering-related processes. In discussions with NASA hypervelocity experts, a representative production relative velocity of ~ 1 km/sec was assumed for the speed of the ejecta. For ORDEM 4.0, a simplified production mechanism was used where the particles, regardless of production mechanism, are ejected randomly in the forward hemisphere with respect to the velocity of the parent body at 1 km/sec. This has a strong effect on the spatial density distribution of these ejecta, as they typically are in elliptical initial orbits with high apogees.

Flux on each STS mission (determined by mission date, orbit, and spacecraft orientation) was computed using the reference population of ejecta, and the size-dependent production rate was adjusted to try to match the feature size distribution of the STS data using a maximum likelihood method, analogous to the radar analysis.

Analysis of small particles from impact ejecta and from other tests indicated that metallic debris at sub-millimeter sizes mostly consisted of “nuggets,” with L:D ratios near “1.” Paint ejecta is modeled, based on high-speed laboratory imagery, to consist of a number of small plates down to a characteristic length similar to typical paint thickness (~ 150 μm), below which they are assumed to be “nuggets.” Because paint particles in the STS database could be uniquely identified, that population was modeled and fitted separately. The damage equations had to be adapted to estimate the feature size of the observed paint craters based on the “disc” (plate-like) and “nugget” assumptions.

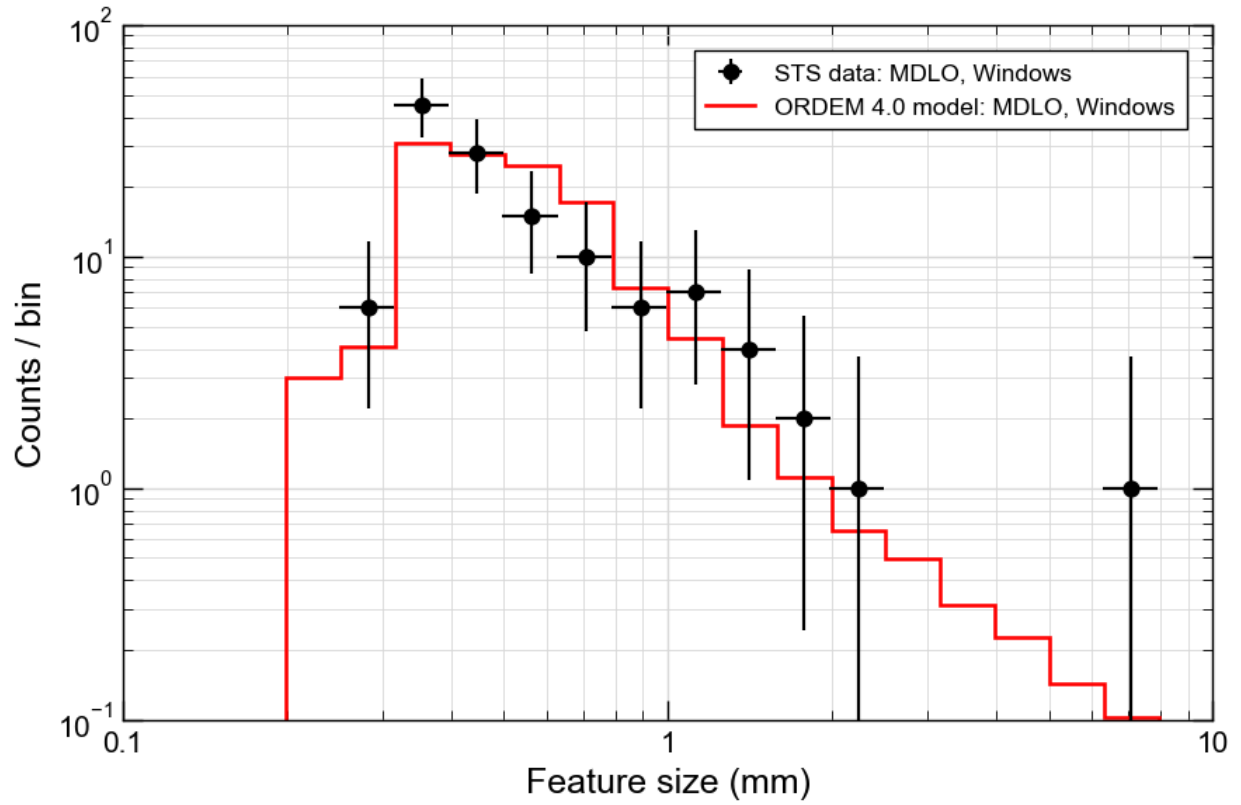


Figure 5. The population based on the Medium-Low density (MDLO – mostly aluminum, paint removed) population fits are predicted to have differential distributions marked in red, and the black dots represent the distribution of STS window damage made by impactors identified as MDLO.

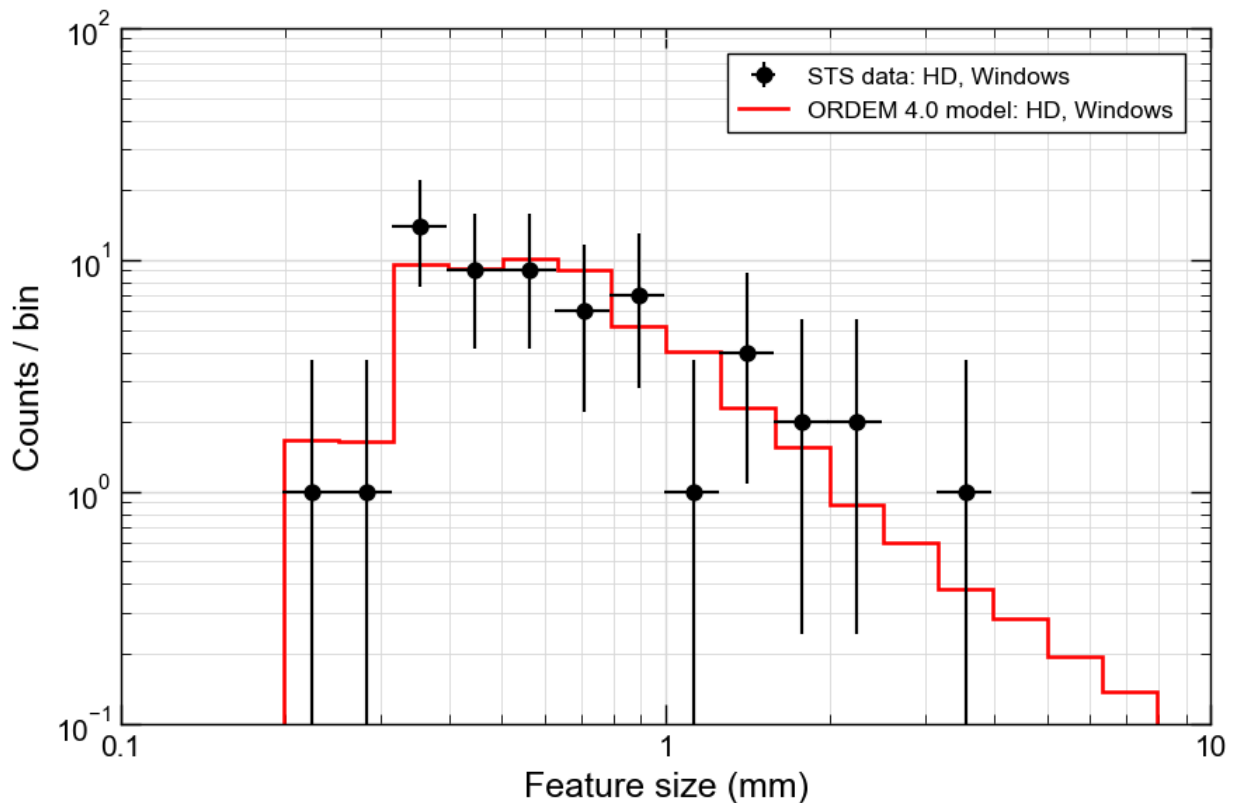


Figure 6. The population based on the High density (HD – mostly steel) population fits are predicted to have differential distributions marked in red, and the black dots represent the distribution of STS window damage made by impactors identified as HD.

Examples of fits are shown in Figs. 5-6. Many of the challenges fitting these small populations are linked to diminishing number of impact features with increasing size. This means that the population in the sizes most critical for spacecraft risk – near 1 mm – have the highest uncertainties. This is also a region where flux and populations change dramatically with size, once again highlighting the need for dedicated, calibrated sensors for consistent modeling of this population.

The primary effect of the high delta-velocity ejecta assumption is in the spatial density distribution with altitude. ORDEM 3.2 small particle populations had spatial densities that varied widely with altitude analogous to the spatial density of the parent body population; however, the new spatial density distribution of these small debris is much flatter at higher altitudes.

In situ data for ORDEM 4.0 validation will include data from the Wide Field Planetary Camera 2 radiator and Hubble Space Telescope (HST) multilayer insulation (MLI) surfaces used for ORDEM 3.1 validation. In addition, new datasets from Pressurized

Mating Adapter-2 blanket surface [22] will be included. The CRS (Commercial Resupply Service) flights, employing the Space Exploration Technologies Corporation (“SpaceX™”) *Dragon*™ capsule, offer a timely and well-characterized source of exposed surfaces. Recent work has demonstrated the feasibility of using samples excised from the capsule’s thermal protective surfaces for impact residue identification; however, additional analysis is required to fully characterize the flux derived from these surfaces due to capsule orientation, passive shielding while docked to the International Space Station (ISS), and sampling methodologies.

4.3 Optical-based Populations

Historically, the Michigan Orbital DEbris Survey Telescope (MODEST) was the ODPO’s primary source of data for debris in GEO from the size limit of the SSN catalog (approximately 1 m) down to approximately 30 cm. Since 2020, NASA’s Eugene Stansbery – Meter Class Autonomous Telescope (ES-MCAT), a 1.3 m telescope located on Ascension Island, has provided GEO survey data for building and

validating ORDEM populations [23]. Objects are filtered to determine those most likely to be GEO debris based on sizes and orbital parameters. In contrast to the radar-based populations, fragmentations are not explicitly included in the ORDEM GEO populations, but are implicitly included directly from the optical data; this approach prevents any potential overestimation of these fragments that are resident in the data. By extension, fragments from any unconfirmed or unknown GEO breakups that have not been modeled are also implicitly included.

For ORDEM 3.1, the MODEST 2004-2006 and 2007-2009 was used to build the GEO population extrapolating from the completeness size of MODEST down to 10 cm in size. Comparisons to MODEST 2013-2014 data during ORDEM 3.1 validation effort resulted in additional fragments being added to the population, including a simulated breakup and additional fragments statistically sampled from the 2013-2014 data. For ORDEM 4.0, the ORDEM 3.1 GEO population was maintained, with an update to extrapolate down to 1 cm, and propagated forward to 2022. Data collected by ES-MCAT during 2020-2022 was compared to the ORDEM 3.1 GEO population predictions during ORDEM 4.0 development. Due to mirror degradation largely driven by effects from the COVID-19 pandemic, this data was deemed incomplete. Data from ES-MCAT observations in 2023 is currently being analyzed for ORDEM 4.0 validation efforts.

5 SUMMARY

The ODPO is currently in the final stages of ORDEM 4.0 development. Most of the architecture has been finalized, and the ORDEM populations have been created. Verification and validation have begun on these populations and the overall model.

The most significant update for ORDEM 4.0 is the inclusion of a shape parameter. The decision to use right circular cylinders to approximate the shapes of debris will result in a major shift in how damage equations are tested, derived, and implemented in spacecraft risk computations, but should greatly improve the accuracy of risk assessments.

Because the environment is dynamic, ORDEM 4.0 uses updated measurements, primarily from ground-based radars such as HUSIR and Goldstone for LEO and ground-based telescopes such as ES-MCAT for GEO. Unfortunately, there are no high-quality, large-area, *in situ* data sources since the cessation of NASA Space Shuttle missions. Therefore, most of the small particle modeling is limited to updated analyses of those data sets, although limited new datasets are used for validation.

6 REFERENCES

1. Kessler, D.J., *et al.* (1989). "Orbital Debris Environment for Spacecraft Designed to Operate in Low Earth Orbit," NASA TM-100 471.
2. Kessler, D.J., *et al.* (1996). "A Computer-Based Orbital Debris Environment Model for Spacecraft Design and Observation in Low Earth Orbit," NASA TM-104 825
3. Liou, J.-C., *et al.* (2002). "The New NASA Orbital Debris Engineering Model ORDEM2000," NASA/TP-2002-210780.
4. Stansbery, E.G., *et al.* (2015). "NASA Orbital Debris Engineering Model ORDEM 3.0 – Verification and Validation," NASA/TP-2015-218592, October.
5. Krisko, P.H. (2014). "The New NASA Orbital Debris Engineering Model ORDEM 3.0," AIAA/AAS Astrodynamics Specialist Conference, 2014-4227.
6. Matney, M., *et al.* "The NASA Orbital Debris Engineering Model 3.1: Development, Verification, and Validation." <https://www.hou.usra.edu/meetings/orbitaldebris2019/orbital2019paper/pdf/6134.pdf>.
7. <https://www.spacecom.mil/Newsroom/News/Article-Display/Article/2842957/russian-direct-ascent-anti-satellite-missile-test-creates-significant-long-last/> (retrieved 1 November 2023).
8. Anon. (2022). "Orbital Debris Engineering Model 3.2 Release." ODQN vol. 26 issue 1, March, p. 5.
9. Seago, J.H., *et al.* (2023). "An Approach to Shape Parameterization Using Laboratory Hypervelocity Impact Experiments." Second International Orbital Debris Conference, Houston, Texas, (<https://www.hou.usra.edu/meetings/orbitaldebris2023/pdf/6145.pdf>).
10. Cowardin, H., *et al.* (2023). "Updates on the Debrisat Hypervelocity Experiment and Characterization of Fragments in Support of Environmental Models," International Journal of Impact Engineering, Volume 180, October, 104669, <https://doi.org/10.1016/j.ijimpeng.2023.104669>.
11. Miller, J., *et al.* (2022). "Development of Experimental Techniques for Non-spherical Hypervelocity Impacts." Proceedings of the 2022 Hypervelocity Impact Symposium. Alexandria, VA, September 18-22.
12. Johnson, N., *et al.* (2001). "NASA's New Breakup Model of EVOLVE 4.0," *Advances in Space Research*, Vol. 28, No. 9 1377-84.

13. Zucker, M., *et al.* (2018). "Cube-to-sphere Projections for Procedural Texturing and Beyond," *Journal of Computer Graphics Techniques*, Vol. 7, No. 2
14. Liou, J.-C., *et al.* (2005). "LEGEND – A Three-Dimensional LEO-to-GEO Debris Evolutionary Model," *Advances in Space Research*, Vol. 34 981-6.
15. Liou, J.-C. (2006). "Collision Activities in the Future Orbital Debris Environment," *Advances in Space Research*, Vol. 38 2102-6.
16. Manis, A., *et al.* (2023). "An Overview of Ground-based Radar and Optical Measurements Utilized by the NASA Orbital Debris Program Office," Second International Orbital Debris Conference, Houston, Texas, (<https://www.hou.usra.edu/meetings/orbitaldebris2023/pdf/6045.pdf>).
17. Arnold, J., *et al.* (2024). Goldstone Radar Measurements of the Orbital Debris Environment: 2020-2021, NASA/TP-20240002199.
18. Hyde, J., *et al.* (2015). "Shuttle MMOD Impact Database." *Procedia Engineering* vol. 103 246-53.
19. Kennedy, T., *et al.* (2022). NASA Orbital Debris Engineering Model ORDEM 3.1 – Model Verification and Validation, NASA/TP-20220002309, NASA Johnson Space Center, Houston, TX, USA.
20. Manis, A., *et al.* (2022). NASA Orbital Debris Engineering Model ORDEM 3.1 – Model Process, NASA/TP-20220004345, NASA Johnson Space Center, Houston, TX, USA.
21. Seago, J., *et al.* "Development of a Model for the Small-Particle Orbital Debris Population Based on the STS Impact Record." (<https://www.hou.usra.edu/meetings/orbitaldebris2019/orbital2019paper/pdf/6137.pdf>).
22. Anz-Meador, P., *et al.* (2023). "A Survey of ISS and Visiting Vehicle Returned Surfaces for Environment Characterization and Computer Model Development." Second International Orbital Debris Conference, Houston, Texas (in press).
23. Cruz, C., *et al.* (2023). "The Completion of a Geosynchronous Earth Orbit Survey with the Eugene Stansbery-Meter Class Autonomous Telescope." Second International Orbital Debris Conference, Houston, Texas, (<https://www.hou.usra.edu/meetings/orbitaldebris2023/pdf/6153.pdf>).